FLUCTUATIONS OF THE ACOUSTIC FIELD BRAGG BACKSCATTERED FROM ROUGH SURFACES

Suzanne T. McDaniel
4035 Luxury Lane
Bremerton, WA 98311

Interim Report
Contract N00014-95-1-0538
January 30, 1996

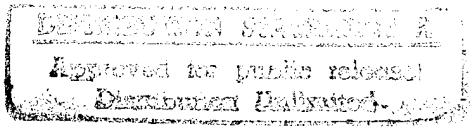

REPORT DOCUMENTATION PAGE

Form Approved
OPM No. 0704-0188

1. AGENCY USE ONLY *(Leave blank)*	2. REPORT DATE	3. REPORT TYPE AND DATES COVERED
	January 1996	Technical

4. TITLE AND SUBTITLE

Fluctuations of The Acoustic Field Bragg Backscattered from Rough Surfaces

5. FUNDING NUMBERS

N00014-95-1-0538

6. AUTHOR(S)

Suzanne T. McDaniel

7. PERFORMING ORGANIZATION NAME(S) AND ADDRESS(ES)

Suzanne T. McDaniel
4035 Luxury Lane
Bremerton, WA 98311

8. PERFORMING ORGANIZATION REPORT NUMBER

9. SPONSORING / MONITORING AGENCY NAME(S) AND ADDRESS(ES)

Office of Naval Research
800 N. Quincy Street
Arlington, VA 22217

10. SPONSORING / MONITORING AGENCY REPORT NUMBER

11. SUPPLEMENTARY NOTES

12a. DISTRIBUTION / AVAILABILITY STATEMENT

Distribution Unlimited

12b. DISTRIBUTION CODE

13. ABSTRACT *(Maximum 200 words)*

A rigorous theory of backscattering from slightly rough statistically nonstationary surfaces is developed. The development procedes through the application of two ensemble averages: the first to all realizations of the surface having fixed nonstationary features, and the second over all nonstationary surface characteristics. The resulting theory is applied to acoustic seafloor reverberation, where it is found that nonstationarity must be assumed to obtain agreement with observed reverberation fluctuations. The analysis is further extended to the time domain where it is demonstrated that for Bragg scatter, no reduction in the predicted fluctuations occurs for frequency diverse waveforms, thus providing a method of differentiating Bragg scatter from other nonresonant scattering processes.

14. SUBJECT TERMS	15. NUMBER OF PAGES
Seafloor reverberation, rough interface scattering, fluctuations	40
	16. PRICE CODE

17. SECURITY CLASSIFICATION OF REPORT	18. SECURITY CLASSIFICATION OF THIS PAGE	19. SECURITY CLASSIFICATION OF ABSTRACT	20. LIMITATION OF ABSTRACT
Unclassified	Unclassified	Unclassified	SAR

Abstract

A rigorous theory of backscattering from slightly rough statistically nonstationary surfaces is developed. The development procedes through the application of two ensemble averages: the first to all realizations of the surface having fixed nonstationary features, and the second over all nonstationary surface characteristics. The resulting theory is applied to acoustic seafloor reverberation, where it is found that nonstationarity must be assumed to obtain agreement with observed reverberation fluctuations. The analysis is further extended to the time domain where it is demonstrated that for Bragg scatter, no reduction in the predicted fluctuations occurs for frequency diverse waveforms, thus providing a method of differentiating Bragg scatter from other nonresonant scattering processes.

Table of Contents

Page

1. Introduction 1

2. Theoretical development 4

2.1. General formulation 4

2.2. Statistical averages 5

3. Frequency domain scattering 7

3.1. Statistically stationary surfaces 7

3.2. Nonstationary surfaces 10

4. Scattering in the time domain 12

4.1. Pure tone pulses 15

4.2. Spectral representation of nonstationary processes 18

4.3. Frequency diversity 19

5. Comparison with experiment 21

6. Discussion 22

Acknowledgement 23

References 24

List of Figures

Page

Figure 1. Geometry for backscattering from a random rough surface 26

Figure 2. Scintillation index for scatter from statistically stationary surfaces having Gaussian and power-law wave-number spectra 27

Figure 3. Ratio of the scattered intensity to that predicted at the Bragg frequency for scattering from a stationary rough surface characterized by a power-law wave-number spectrum 28

Figure 4. Scintillation index for scattering from rough surfaces having Gaussian and exponentially correlated nonstationarity with a characteristic length of 20 m..... 29

Figure 5. Scintillation index for scattering from rough surfaces having Gaussian and exponentially correlated nonstationarity with a characteristic length of 5 m..... 30

Figure 6. Dependence of the scintillation index on beamwidth for scattering from rough surfaces having Gaussian and exponentially correlated nonstationarity with characteristic lengths of 5 and 20 m 31

Figure 7. Normalized temporal covariance of the impulse response for scatter from a rough surface characterized by power-law wave-number spectra with characteristic lengths of 20 and 100 m 32

Figure 8. Normalized temporal intensity covariance for the scatter of a 1 msec pure tone pulse from a stationary rough surface and surfaces having Gaussian correlated nonstationarity with characteristic length as a parameter 33

Figure 9. Normalized temporal intensity covariance for the scatter of a 10 msec pure tone pulse from a stationary rough surface and surfaces having Gaussian correlated nonstationarity with characteristic length as a parameter 34

Figure 10. Relative predictions of $< p(\tau_s + \Delta t/2)p^*(\tau_s - \Delta t/2) >$ by (17) and its approximation (18) for the scatter of a 1 msec pure tone pulse from a rough surface having a wave-number spectrum of power-law form with a characteristic length of 100 m 35

Figure 11. Comparison of measured scintillation indices as a function of effective pulse length with that predicted assuming Gaussian correlated nonstationarity 36

1. Introduction

The scintillations of signals propagated through turbulence or scattered from rough surfaces, such as the twinkling of stars or the play of sunlight on water, have long fascinated man. As a consequence, extensive research has been devoted to first understanding and explaining such phenomena and subsequently to exploiting them to probe the environment. Despite these efforts, the nature of the reverberant field backscattered from rough surfaces at low grazing angles is still poorly understood.

An analogy is often drawn between rough surface scatter and scattering from a random distribution of discrete points [Goodman 1976]. In this case, the scattered field is regarded as the complex sum of the contributions from the many elementary areas of the surface that are simultaneously irradiated. If the contributions from each scattering element are independent and their phase is uniformly distributed over its full range, then, as the number of such areas becomes large the distribution of the amplitude of the scattered field approaches the Rayleigh distribution. In this article, the scintillation index, which is unity for the Rayleigh distribution, is used as a measure of the strength of the fluctuations.

Measured statistics of microwave sea surface clutter and of acoustic seabed reverberation are generally found to exhibit significantly higher fluctuations than those predicted by the Rayleigh distribution. A number of approaches have been taken to model or explain these phenomena. Jakeman and Pusey [1976] and Oliver [1983] propose models that basically stem from a consideration of point scattering theory. To explain the fluctuations of seafloor reverberation, Crowther [1980] modeled the seabed scattering strength as a two-valued random variable, and McDaniel [1990] treated seabed reverberation as a spectral estimation process. None of these approaches follow from a rigorous consideration of rough surface scattering theory. An exception is the study of Valenzuela and Laing [1970] who applied composite-roughness theory [Kur'ynov 1963] to radar scattering from the sea surface. They found, however, that such effects were insufficient to explain the observed fluctuations.

This study addresses the fluctuations of seafloor reverberation at acoustic frequencies in

the kHz regime. The basic assumptions invoked are first that penetration into the seabed with subsequent rescattering may be neglected, and second that the seafloor is slightly rough so that scattering may be treated using the small waveheight approximation. The first of these assumptions restricts the applicability of the theory to the sandy seabeds [Jackson and Briggs 1992] that are characteristic of the shallow water areas of continental shelves. The second requires that the Rayleigh parameter be small. For a plane wave incident on a slightly rough surface that contains roughnesses of all length scales, the small waveheight approximation predicts that the backscattered field depends only on that surface component having a wave number $K_B = k_x/2$ where k_x is the horizontal component of the incident wave vector. However, for the directional sources used in reverberation measurements, backscatter is governed by a range of surface wave numbers about the Bragg wave number K_B. The range of rough surface wave numbers contributing to the scatter is found to play an important role in determining fluctuation statistics.

With these two assumptions, a rigorous theory is developed to predict the scintillation index and scattered intensity covariance of backscatter. A general treatment is developed for statistically nonstationary surfaces: surfaces for which the correlation of the rough surface excursion at two separated points $\vec{\rho}_1$ and $\vec{\rho}_2$ depends on both $\vec{\rho}_1$ and $\vec{\rho}_2$ as opposed to the stationary case where the correlation depends only on the separation $(\vec{\rho}_1 - \vec{\rho}_2)$. The key to this development is the application of two ensemble averages: the first to that set of surfaces having a fixed or deterministic nonstationary character, and the second over all possible realizations of nonstationary characteristics. The general theoretical formulation of the problem and definition of the statistical averaging procedures for stationary and nonstationary surface repesentations are presented in section 2.

Section 3.1 addresses frequency domain scattering from statistically stationary surfaces. Assuming a simple form for the source directivity, the scintillation index is found to be identical to the Rayleigh value of unity provided that the dimensions of the ensonified area are large on a wavelength scale and the rough surface wave-number spectrum (the spatial

Fourier decomposition of the surface correlation function) is slowly varying in the vicinity of the Bragg wave number. These two provisions insure that only a small range of rough surface wave numbers contribute to the scatter and are furthermore consistent with the geometries employed in seafloor reverberation measurements and also with the applicable measurements of seabed roughness wave-number spectra [Briggs 1989]. Section 3.2 extends the frequency domain treatment to statistically nonstationary surfaces. Two very simple representations of the nonstationary process are assumed, both of which yield similar results and predict the one clear trend, a significant increase in fluctuations with decreasing ensonified surface area, that is indicated by the available statistical data [Crowther 1980, Chotiros et al 1985, Boehme and Chotiros 1988, and Gensane 1989].

In section 4, the theory is extended to the time domain, where it is found that to obtain results independent of the specific form of the surface correlation function, the surface wave-number spectrum must again be slowly varying in the vicinity of the Bragg wave number. To obtain a formulation amenable to numerical analysis, an additional approximation is made that limits the validity of the results to waveforms of moderate bandwidth. Results for the scintillation index and time-lagged intensity covariance are obtained for pure tone pulses, and it is demonstrated that the intensity covariance may be inverted to estimate the spatial structure of nonstationary surface features.

Section 4.3 addresses frequency diversity effects, whereby significant reductions of the scintillation index have been experimentally obtained [Ulaby, et al 1988, George and Jain 1972] by increasing the time-bandwidth product of the waveform used above its nominal value of unity for a pure tone pulse. For the backscatter process considered here, a frequency diversity effect is not predicted for either stationary or nonstationary surface statistics, given the conditions under which the theory is valid. This is an important finding because it represents a means of experimentally differentiating between Bragg scatter and other scattering mechanisms, such as volume scatter, that exhibit a frequency diversity effect.

In section 5, predicted scintillation indices are compared with the data of Gensane [1989]

using a simple two parameter model for the nonstationary surface features. Agreement is obtained with the data by assuming that the normalized variance of the surface roughness wave-number spectrum is approximately unity, and that the characteristic length scale of nonstationary surface features is on the order of 1 m.

In section 6, the major findings of this study are summarized: that nonstationary surface statistics must be assumed to account for experimental observations, and that frequency diversity effects do not occur for Bragg backscatter. Other nonstationary features of the seafloor that may affect fluctuation statistics are also discussed.

2. Theoretical development

2.1. General formulation

The scattering geometry considered is depicted in figure 1, in which the acoustic field incident from a directional source is backscattered from a rough surface. The backscattered acoustic pressure $p(t)$ obeys

$$p(t) = \int_{-\infty}^{\infty} h(\tau) e(t-\tau) d\tau \tag{1}$$

where $h(\tau)$ is the impulse response of the scattering channel, and $e(t)$ is the transmitted waveform. The impulse response is related to the frequency response $H(\omega)$ by a Fourier transform

$$H(\omega) = \int_{-\infty}^{\infty} d\tau h(\tau) \exp(-i\omega\tau) \tag{2}$$

For a backscattering geometry, the Fraunhofer phase is large, so that Fresnel phase corrections [Melton and Horton 1970] may be neglected, and the applicable expression for a slightly rough surface is

$$H(\omega) = F \int d\vec{\rho}_1 \zeta_1 \exp[i\omega(\tau_s - \alpha x_1)] \, \Omega_1 \tag{3}$$

where

$$F = \omega^2 \chi(\theta) \sin^2\theta / (\pi R^2 c^2) \tag{4}$$

$$\alpha = 2\cos\theta / c$$

and $\chi(\theta)$ is a modified reflection coefficient [Jackson, et al, 1986], $\Omega_1 = \Omega(\vec{\rho}_1)$ is the surface ensonification function, $\tau_s = 2R/c$ is the two way travel time from the source to the origin of the coordinate system, with c the sound speed in the host medium, and ω the radian frequency. The grazing angle θ, slant range R, and excursion of the rough surface from its mean value $\zeta_1 = \zeta(\vec{\rho}_1)$ that appear in these expressions are depicted in figure 1. In obtaining this expression for $H(\omega)$ it has been assumed that R, θ and χ may be considered constant over the ensonified area.

In the expression for $H(\omega)$ given above, only its dependence on the stochastic parameter ζ_1 has been made explicit. The body of this article addresses the dependence of intensity moments on this parameter. However, the modified reflection coefficient $\chi(\theta)$ may also vary with position through its dependence on the local values of sediment properties. The derivation for this case closely follows that for stochastic variations of ζ and will be discussed later. From the viewpoint of composite-roughness theory, $H(\omega)$ also depends on the local large-scale surface slope, through which the grazing angle θ may be considered a stochastic variable. Valenzuela and Laing [1970] investigated this effect for the scattering of radar waves from the sea surface and concluded that it was insufficient to explain the experimentally observed fluctuations. Because the slopes of horizontally large-scale seafloor elevations are considerably lower than those of the sea surface, this effect is not considered.

2.2. Statistical averages

Our interest is in determining the expected value of moments of the received pressure field, namely $< p(t)p^*(t) >$ and $< p(t)p^*(t)p(t')p^*(t') >$. From expressions (1) and (3), it is apparent that these expected values depend on the second and fourth moments of the rough surface excursion $< \zeta_1\zeta_2 >$ and $< \zeta_1\zeta_2\zeta_3\zeta_4 >$. For a statistically stationary surface

$$< \zeta_1\zeta_2 >= C(\vec{\rho}_1 - \vec{\rho}_2) = \int d\vec{K} W(\vec{K}) \exp[i\vec{K} \cdot (\vec{\rho}_1 - \vec{\rho}_2)] \tag{5}$$

In this case the correlation function C depends only on the separation $\vec{\rho}_1 - \vec{\rho}_2$, with the surface roughness wave-number spectrum $W(\vec{K})$ being defined as the spatial Fourier transform of C.

If the rough surface is statistically nonstationary $< \zeta_1 \zeta_2 >$ takes the form [Papoulis, 1965]

$$< \zeta_1 \zeta_2 >= C(\vec{\rho}_1, \vec{\rho}_2)$$

With the change of variables $\vec{\rho}_- = \vec{\rho}_1 - \vec{\rho}_2$ and $\vec{\rho}_+ = (\vec{\rho}_1 + \vec{\rho}_2)/2$, a position dependent surface roughness wave-number spectrum $W(\vec{K}, \vec{\rho}_+)$ can be defined

$$< \zeta_1 \zeta_2 >= C(\vec{\rho}_-, \vec{\rho}_+) = \int d\vec{K} W(\vec{K}, \vec{\rho}_+) \exp i\vec{K} \cdot \vec{\rho}_- \tag{6}$$

in analogy to the definition of the wave-number spectrum for a stationary rough surface. The wave-number spectrum $\overline{W}(\vec{K})$ averaged over all nonstationary realizations of the rough surface, where the overbar is used to designate this average, is defined as

$$\overline{W}(\vec{K}) = \lim_{x_+, y_+ \to \infty} \int_{-x_+}^{x_+} \int_{-y_+}^{y_+} \frac{d\vec{\rho}_+}{4 x_+ y_+} W(\vec{K}, \vec{\rho}_+)$$

Let us now return to the problem at hand, the estimation of such quantities as

$$< H(\omega) H^*(\omega) >= |F|^2 \int d\vec{\rho}_- d\vec{\rho}_+ d\vec{K} W(\vec{K}, \vec{\rho}_+) \Omega_1 \Omega_2 \exp\{i[\vec{K} \cdot \vec{\rho}_- - \omega\alpha(x_1 - x_2)]\}$$

The ensonification factors Ω_1 and Ω_2 in this expression determine the extent of the integration over $\vec{\rho}_+$. This integration then yields a *local average* of the position dependent wave-number spectrum over the ensonified area. Thus, to obtain the expectation of $H(\omega)H^*(\omega)$ for all nonstationary representations of the rough surface, an additional ensemble average corresponding to that performed to obtain $\overline{W}(\vec{K})$ is necessary

$$< \overline{H(\omega) H^*(\omega)} >= |F|^2 \int d\vec{\rho}_- d\vec{\rho}_+ d\vec{K} \overline{W}(\vec{K}) \Omega_1 \Omega_2 \exp\{i[\vec{K} \cdot \vec{\rho}_- - \omega\alpha(x_1 - x_2)]\}$$

The procedure described above for determining the expected moments of the rough surface excursion entails two ensemble averages. The first is over all realizations of the surface having the same nonstationary characteristics. An example of such a set of surfaces is an ensemble in which the rms roughness varies deterministically with position. The second ensemble average is over all nonstationary realizations of the suface. For the example considered, this second average is over all possible variations of the rms roughness with position.

Obtaining second moments of the scattered intensity entails evaluating the fourth moment of the rough surface excursion $< \zeta_1\zeta_2\zeta_3\zeta_4 >$. If ζ is a Gaussian random variable

$$< \zeta_1\zeta_2\zeta_3\zeta_4 >=< \zeta_1\zeta_2 >< \zeta_3\zeta_4 > + < \zeta_1\zeta_3 >< \zeta_2\zeta_4 > + < \zeta_1\zeta_4 >< \zeta_3\zeta_2 > \qquad (7)$$

It follows from the result obtained above for $< \overline{\zeta_1\zeta_2} >$ that the ensemble average over all nonstationary surfaces of a representative term on the right hand side of (7) takes the form

$$< \overline{\zeta_1\zeta_2} >< \overline{\zeta_3\zeta_4} >= \int d\vec{K}d\vec{K}'\overline{W(\vec{K},\vec{\rho}_+)W(\vec{K}',\vec{\rho}'_+)}\exp[i\vec{K}\cdot(\vec{\rho}_1-\vec{\rho}_2)+i\vec{K}'\cdot(\vec{\rho}_3-\vec{\rho}_4)]$$

where $\vec{\rho}'_+ = (\vec{\rho}_3+\vec{\rho}_4)/2$.

If $\overline{W}(\vec{K})$ for a nonstationary surface is chosen equal to $W(\vec{K})$ for a stationary surface, then the mean intensity scattered in the two cases will be identical. However, the above expression for the fourth moment of ζ depends on the correlation function of $W(\vec{K},\vec{\rho})$ at disjoint positions, so that the second moment of the intensity will, in general, differ in the two cases.

3. Frequency domain scattering

It is clear that obtaining numerical results from the theoretical formulation of section 2 presents some difficulty. It is hence useful to first examine scattering in the frequency domain to establish the validity of the various approximations that are needed to obtain results amenable to numerical analysis.

3.1. Statistically stationary surfaces

To obtain results for the statistically stationary case, it will be assumed that the projector ensonification function Ω is Gaussian

$$\Omega_1 = \exp[-x_1^2/(\Delta x)^2 - y_1^2/(\Delta y)^2] \qquad (8)$$

where

$$\Delta x = gR\tan(\phi_x/2)/\sin\theta$$

$$\Delta y = gR\tan(\phi_y/2)$$

with ϕ_x and ϕ_y the projector half-power beam widths along the x and y axes, respectively, and $g = [2/\ln(2)]^{1/2}$. The ensonified area in this case is given by $\pi\Delta x\Delta y/2$.

For this form of the ensonification function, $< I(\omega) >=< H(\omega)H^*(\omega) >$ is given by

$$< I(\omega) >= |F|^2 \int d\vec{\rho}_+ d\vec{\rho}_- d\vec{K} W(\vec{K}) \exp[i(\vec{K}\cdot\vec{\rho}_- - \omega\alpha x_-)]$$

$$\times \exp[-\frac{2x_+^2 + x_-^2/2}{(\Delta x)^2} - \frac{2y_+^2 + y_-^2/2}{(\Delta y)^2}]$$

where $\vec{\rho}_- = (x_-, y_-)$ and $\vec{\rho}_+ = (x_+, y_+)$. The integrals over $\vec{\rho}_-$ and $\vec{\rho}_+$ in this expression may be immediately performed to obtain

$$< I(\omega) >= |F|^2\pi^2(\Delta x\Delta y)^2 \int d\vec{K} W(\vec{K}) \exp[-(K_x - \alpha\omega)^2(\Delta x)^2/2 - K_y^2(\Delta y)^2/2]$$

The remaining integral over $\vec{K}$ is an average of $W(\vec{K})$ about the Bragg wave number $\vec{K}_B = (\alpha\omega, 0)$. With the definition

$$W_B = \Delta x\Delta y \int \frac{d\vec{K} W(\vec{K})}{2\pi} \exp[-(K_x - \alpha\omega)^2(\Delta x)^2/2 - K_y^2(\Delta y)^2/2]$$

the mean scattered intensity takes the form

$$< I(\omega) >= 2\pi^3 |F|^2 (\Delta x\Delta y) W_B \tag{9}$$

It should be noted that for wave-number spectra that are strongly varying functions of $\vec{K}$, W_B may differ significantly from $W(\vec{K}_B)$. With the same approximations, the second moment of the intensity is given by

$$< I^2(\omega) >= 2 < I(\omega) >^2 \tag{10}$$

$$+\{|F|^2\pi^2(\Delta x\Delta y)^2 \int d\vec{K} W(\vec{K}) \exp[-(K_x^2 + \alpha^2\omega^2)(\Delta x)^2/2 - K_y^2(\Delta y)^2/2]\}^2$$

The expressions developed above for the first and second moments of the backscattered intensity will be evaluated for two assumed forms of the wave-number spectrum $W(\vec{K})$. The first is the Gaussian form that is often assumed in scattering problems because of its ease of numerical implementation

$$W(\vec{K}) = S \exp[-(K_x^2 + K_y^2)L^2]$$

where L is a characteristic length, and S a scale factor. For this wave-number spectrum,

$$W_B = S\{[1 + 2(L/\Delta x)^2][1 + 2(L/\Delta y)^2]\}^{-1/2} \exp\{-(\alpha\omega L)^2/[1 + 2(L/\Delta x)^2]\}$$

It is evident from this expression, that for $L \gg \Delta x$, W_B will greatly exceed $W(\vec{K}_B) = S\exp[-(\alpha\omega L)^2]$. In such cases, a broad range of wave numbers contributes to W_B, and the scattering process differs from classical view of Bragg diffraction as wave-number selective.

For the Gaussian spectrum, the scintillation index $\sigma^2 = [< I^2(\omega) > / < I(\omega >^2] - 1$ takes the form

$$\sigma^2 = 1 + \exp\{-(\alpha\omega\Delta x)^2/[1 + 2(L/\Delta x)^2]\}$$

It is clear from this result that for a Gaussian spectrum, σ^2 depends strongly on frequency, a dependence that has not been observed experimentally. This result is also independent of Δy the cross-range extent of the ensonified area.

The second surface wave-number spectrum that will be considered is more typical of those associated with the seafloor [Briggs 1989, Fox and Hayes 1985, Goff and Jordan 1988]

$$W(\vec{K}) = S/[1 + L^2(K_x^2 + K_y^2)] \tag{11}$$

The numerical evaluation of W_B and σ^2 for this wave-number spectrum may be simplified by the use of the formula [Gradshteyn and Ryzhik 1980]

$$\int_0^\infty \frac{dv \exp[-(\mu v)^2]}{(v^2 + \beta^2)} = \pi[1 - \Phi(\beta\mu)] \exp[(\beta\mu)^2]/(2\beta)$$

where Φ is the probability function, to perform the integrations over K_y.

The scintillation index predicted for the power-law spectrum is compared with that for the Gaussian wave-number spectrum in figure 2. In this example, the grazing angle θ is 30°, the frequency 10 kHz, and the characteristic length L is 20 m. For the narrow beam patterns assumed $\phi_x = \phi_y = 1°$, the dimensions of the ensonified area do not exceed L even for the longest range considered. The results presented in figure 2 parallel those obtained by Yang, Fennemore and McDaniel [1992] for forward scattering. They found that strong fluctuations

occured only when the source or receiver was in the near field of the surface, and that these fluctuations were stronger for a Gaussian wave-number spectrum than for a quasipower-law spectrum. They also found that the introduction of an ensonification function led to higher fluctuations.

For the extreme example considered in figure 2, W_B predicted by the Gaussian wave-number spectrum exceeds $W(\vec{K}_B)$ by many orders of magnitude. The ratio $W_B/W(\vec{K}_B)$ is shown for the power-law spectrum in figure 3. Only at the very shortest ranges does this ratio differ significantly from unity. It is apparent from the results of this subsection that if we restrict our interest to wave-number spectra that are slowly varying in the neighborhood of the Bragg wave number, and to ensonification functions such that Δx and Δy are large on a wavelength scale, the scintillation index will be unity for scattering from stationary surfaces.

3.2. Nonstationary surfaces

For the nonstationary case, the derivation closely follows that for the stationary case. With the introduction of a Gaussian beam pattern, the mean intensity for a nonstationary representation of the rough surface may readily be reduced to the form

$$< I(\omega) >= 4\pi^2|F|^2 \int d\vec{\rho}_+ W_B(\vec{\rho}_+) \exp[-2x_+^2/(\Delta x)^2 - 2y_+^2/(\Delta y)^2]$$

where

$$W_B(\vec{\rho}_+) = \Delta x \Delta y \int \frac{d\vec{K} W(\vec{K}, \vec{\rho}_+)}{2\pi} \exp[-(K_x - \alpha\omega)^2(\Delta x)^2/2 - K_y^2(\Delta y)^2/2]$$

An ensemble average over all nonstationary surfaces then yields

$$\overline{< I(\omega) >} = 2\pi^3|F|^2(\Delta x \Delta y) W_B$$

where it has been assumed that $\overline{W}_B(\vec{\rho}_+) = W_B$.

It is clear from the results of setion 3.1 that for cases of practical interest $< I^2(\omega) >$ may be approximated by $2 < I(\omega) >^2$. Performing an average over all nonstationary representations of the surface then yields

$$\overline{< I^2(\omega) >} = 2\overline{< I(\omega) >< I(\omega) >}$$

$$\overline{< I^2(\omega) >} = 2(2\pi)^4 |F|^4 \int d\vec{\rho}_+ d\vec{\rho}'_+ \overline{W_B(\vec{\rho}_+) W_B(\vec{\rho}'_+)}$$
$$\times \exp[-2(x_+^2 + x_+'^2)/(\Delta x)^2 - 2(y_+^2 + y_+'^2)/(\Delta y)^2]$$

Because $W_B(\vec{\rho}_+)$ and $W_B(\vec{\rho}'_+)$ entail an average over a narrow band of wave numbers about the Bragg wave number for wave-number spectra of interest, their correlation function will be assumed to depend on position alone.

To evaluate the expression for $\overline{< I^2(\omega) >}$ the two position wave-number correlation function is assumed to be of the general form

$$\overline{W_B(\vec{\rho}_+) W_B(\vec{\rho}'_+)} = W_B^2[1 + \gamma C_W(\vec{\rho}_+ - \vec{\rho}'_+)] \tag{12}$$

where γ is the normalized variance of the wave-number spectrum and C_W is a normalized correlation function. Using this form for the correlation function in the expression for $< \overline{I^2(\omega) >}$, thence making the change of variables $\vec{u} = \vec{\rho}_+ - \vec{\rho}'_+$, $\vec{U} = (\vec{\rho}_+ + \vec{\rho}'_+)/2$, the scintillation index may be reduced to

$$\sigma^2 = 1 + \int \frac{2\gamma \, d\vec{u}}{\pi \Delta x \Delta y} C_W(\vec{u}) \exp[-\frac{u_x^2}{(\Delta x)^2} - \frac{u_y^2}{(\Delta y)^2}]$$

Crowther [1980] modeled scattering from a seafloor consisting of random patches taking on only two values of the scattering strength: a low scattering strength with probability s and a high scattering strength with probability $1 - s$. Assuming a ratio of high to low scattering strengths ν, he found $\gamma = s(1-s)(\nu-1)^2/[1 + s(\nu-1)]^2$ and that C_W was exponentially distributed

$$C_W(\vec{u}) = \exp(-|\vec{u}|/L_W)$$

where L_W characterizes the patch size. Inserting this correlation function in the expression for σ^2 and making the change of variables $u_x = r\cos\psi$, $u_y = r\sin\psi$, yields

$$\sigma^2 = 1 + \int_0^\infty \frac{2\gamma \, r dr}{\pi \Delta x \Delta y} \int_0^{2\pi} d\psi \exp[-r^2 f(\psi) - r/L_W]$$

where $f(\psi) = \sin^2\psi/(\Delta x)^2 + \cos^2\psi/(\Delta y)^2$. The integration over r in this expression may be readily performed. The remaining integral over ψ can then be evaluated numerically.

To examine the sensitivity of the scintillation index to the assumed form of the correlation function the Gaussian case will also be considered

$$C_W(\vec{u}) = \exp[-(u_x^2 + u_y^2)/L_W^2] \tag{13}$$

For this correlation function,

$$\sigma^2 = 1 + 2\gamma/\{[1 + (\Delta x/L_W)^2][1 + (\Delta y/L_W)^2]\}^{1/2}$$

It is apparent from this result that $1 \leq \sigma^2 \leq 1+2\gamma$, with the maximum value being obtained when L_W is much larger than the dimensions of the ensonified area.

The results obtained above for the scintillation index display no explicit dependence on frequency. However, such a dependence is implicit because $W_B(\vec{\rho}_+)$ and its correlation depend on the Bragg wave number $\vec{K}_B = (\alpha\omega, 0)$.

The scintillation indices predicted for the exponential and Gaussian correlation functions are compared in figure 4 which shows their dependence on slant range for a fixed grazing angle 30° and beam pattern $\phi_x = \phi_y = 10°$. In this example, $\gamma = .25$ and $L_W = 20$ m. The results for the exponential and Gaussian correlation functions are in close agreement and approach unity as the slant range increases, and the dimensions of the ensonified area approach the characteristic length L_W. This decrease in the scintillation index is more evident in figure 5 which shows corresponding results for $L_W = 5$ m. In this figure, the results obtained for the two correlation functions are again in close agreement.

Figure 6 shows the dependence of σ^2 on ϕ_x for a fixed grazing angle of 30° for two values of the characteristic length: the remaining parameters are those used in figure 5. Again, the predicted scintillation index decreases as the size of the ensonified area increases. In this example, clear differences in the predictions of the Gaussian and exponential models are evident for very small beamwidths.

4. Scattering in the time domain

In most backscattering experiments the resolution in range is determined by the length of the transmitted pulse and the effect of the beam pattern on range resolution is negligible.

Hence, in obtaining results in the time domain $\Omega(x,y)$ will be replaced by $\Omega(y)$ in the analysis.

An additional approximation will be made to simplify the analysis: that the scattering is *frequency independent.* With this assumption the function F is approximated by $\omega_0^2\chi(\theta)\sin^2\theta/(\pi R^2c^2)$ where ω_0 is the center frequency of the transmitted pulse. While this approximation is consistent with those made to approximate other factors in F that do not appear in the argument of an exponential by their mean values, it is evident that it limits the validity of the results to waveforms of moderate bandwidth.

Following the general formulation developed in section 2, one finds

$$h(\tau) = F\int dx_1 dy_1 \delta(\tau - \tau_s - x_1\alpha)\exp[-y_1^2/(\Delta y)^2]\zeta_1$$

and consquently that

$$p(t) = F\int dx_1 dy_1 \zeta_1 \exp[-y_1^2/(\Delta y)^2]e[t-(\tau_s + x_1\alpha)]$$

For statistically nonstationary surfaces, it follows that

$$< p(t)p^*(t') >= |F|^2 \int d\vec{\rho}_- d\vec{\rho}_+ d\vec{K} W(\vec{K},\vec{\rho}_+)\exp[-(y_1^2+y_2^2)/(\Delta y)^2]$$
$$\times \exp(i\vec{K}\cdot\vec{\rho}_-)e[t-(\tau_s+x_1\alpha)]e^*[t'-(\tau_s+x_2\alpha)] \qquad (14)$$

Irrespective of the frequency independent approximation used to obtain (14) the time-lagged intensity covariance is given by

$$< I(t)I(t') >=< p(t)p^*(t) >< p(t')p^*(t') > + < p(t)p^*(t') >< p(t')p^*(t) > \qquad (15)$$

where the only assumption made to obtain this result is that an additional term $< p(t)p(t') >$ $< p^*(t)p^*(t') >$ appearing in this expression may be neglected, as demonstrated in section 3.

Before considering specific waveforms, it is worthwhile obtaining general results for statistically stationary surfaces to determine if any approximations that simplify the analysis may be obtained. First consider

$$< h(\tau)h^*(\tau') >= |F|^2 \int d\vec{\rho}_1 d\vec{\rho}_2 \delta(\tau - \tau_s - x_1\alpha)\delta(\tau' - \tau_s - x_2\alpha)$$

$$\times \exp[-(y_1^2 + y_2^2)/(\Delta y)^2] C(\vec{\rho}_1 - \vec{\rho}_2) \tag{16}$$

Replacing $C(\vec{\rho}_1 - \vec{\rho}_2)$ by its Fourier decomposition in wave-number space, the result obtained is

$$< h(\tau)h^*(\tau') >= (|F|/\alpha)^2 \int dy_+ dy_- d\vec{K} W(\vec{K})$$

$$\times \exp[-(2y_+^2 + y_-^2/2)/(\Delta y)^2 + iK_x(\tau - \tau')/\alpha + iK_y y_-]$$

Performing the integrals over y_+ and y_- in this expression, then yields

$$< h(\tau)h^*(\tau') >= \pi(\Delta y|F|/\alpha)^2 \int d\vec{K} W(\vec{K}) \exp[iK_x(\tau - \tau')/\alpha - K_y^2(\Delta y)^2/2]$$

This integral may be readily evaluated numerically. Normalized results are shown in figure 7 for the power-law spectrum (11) for two values of the characteristic length L. It is evident from this figure, that the temporal covariance of the impulse response is a slowly varying function of lag time for the time scales of interest. It is also apparent that this function is dependent on the characteristic length L, as is strongly suggested by the representation (16).

Because consideration of the time-lagged covariance of the impulse response fails to yield any obvious simplifications, we next address

$$< p(\tau_s + \Delta t/2)p^*(\tau_s - \Delta t/2) >= |F|^2 \int d\vec{\rho}_- d\vec{\rho}_+ d\vec{K} W(\vec{K}) \exp(i\vec{K} \cdot \vec{\rho}_-)$$

$$\times \exp[-(2y_+^2 + y_-^2/2)/(\Delta y)^2] e(\Delta t/2 - x_1\alpha) e^*(-\Delta t/2 - x_2\alpha)$$

where t and t' have been replaced by $\tau_s + \Delta t/2$ and $\tau_s - \Delta t/2$, respectively, and stationary surface statistics have been assumed. Performing the integrals over y_+ and y_-, and substituting $e(\Delta t/2 - x_1\alpha) = \hat{e}(\Delta t/2 - x_1\alpha) \exp[i\omega_0(\Delta t/2 - x_1\alpha)]$, where $\hat{e}$ is the complex signal envelope, along with the corresponding relation for $e(-\Delta t/2 - x_2\alpha)$, into this expression yields

$$< p(\tau_s + \Delta t/2)p^*(\tau_s - \Delta t/2) >= \pi|F|^2(\Delta y)^2 \int dU dK_y dx_1 dx_2 W(U + \alpha\omega_0, K_y)$$

$$\times \exp[-K_y^2(\Delta y)^2/2 + iU(x_1 - x_2) + i\omega_0\Delta t] \hat{e}(\Delta t/2 - x_1\alpha) \hat{e}^*(-\Delta t/2 - x_2\alpha) \tag{17}$$

where $U = K_x - \alpha\omega_0$. If it is now assumed that $W(U + \alpha\omega_0, K_y)$ varies so slowly with U that this dependence may be neglected, the integral over U yields $2\pi\delta(x_1 - x_2)$, and

$$< p(\tau_s + \Delta t/2)p^*(\tau_s - \Delta t/2) >= 2\pi^2|F|^2(\Delta y)^2 \exp(i\omega_0\Delta t)$$

$$\times \int dx_+ \hat{e}(\Delta t/2 - x_+\alpha)\hat{e}^*(-\Delta t/2 - x_+\alpha) \int dK_y W(\alpha\omega_0, K_y) \exp[-K_y^2(\Delta y)^2/2] \qquad (18)$$

The analagous approximation for nonstationary surfaces takes the form

$$< p(\tau_s + \Delta t/2)p^*(\tau_s - \Delta t/2) >= (2\pi)^2|F|^2 \exp(i\omega_0\Delta t)$$

$$\times \int dx_+ \hat{e}(\Delta t/2 - x_+\alpha)\hat{e}^*(-\Delta t/2 - x_+\alpha) \int dy_+ \widetilde{W}_B(\vec{\rho}_+) \exp[-2y_+^2/(\Delta y)^2] \qquad (19)$$

where $\widetilde{W}_B(\vec{\rho}_+)$ is defined as

$$\widetilde{W}_B(\vec{\rho}_+) = \Delta y/(2\pi)^{1/2} \int dK_y W[(\alpha\omega_0, K_y), \vec{\rho}_+] \exp -K_y^2(\Delta y)^2/2$$

It is clear that (18) could also be obtained by assuming that $< h(\tau)h^*(\tau') >$ of (16) contains a factor $\delta(\tau - \tau')$ which is the case for point scatterers [Ol'shevskii 1967]. However, we have seen that $< h(\tau)h^*(\tau') >$ is in general a slowly varying function of $\tau - \tau'$ and hence such an assumption is useful for rough surface scatter only if the surface roughness wave-number spectrum is a slowly varying function of K_x near $K_x = \alpha\omega_0$.

4.1. Pure tone pulses

The expressions above will first be evaluated for a Gaussian weighted pure tone pulse

$$e(t - \tau) = \exp[i\omega_0(t - \tau) - (t - \tau)^2/T^2] \qquad (20)$$

for which the half-power, or effective, pulse length T_p is given by $(2\ln 2)^{1/2}T$. First, we consider the scintillation index, which entails evaluation of $< p(\tau_s)p^*(\tau_s) >$. Proceeding directly to the case of statistically nonstationary surfaces one readily finds

$$< p(\tau_s)p^*(\tau_s) >= 4\pi^2|F|^2 \int d\vec{\rho}_+ \widehat{W}_B(\vec{\rho}_+) \exp[-2y_+^2/(\Delta y)^2 - x_+^2\alpha^2/T^2]$$

where

$$\widehat{W}_B(\vec{\rho}_+) = (\Delta y T/2\pi\alpha) \int d\vec{K} W(\vec{K}, \vec{\rho}_+) \exp[-K_y^2(\Delta y)^2/2 - (K_x - \alpha\omega_0)^2T^2/(2\alpha^2)]$$

On comparing this result with the comparable result for $< I(\omega) >$ obtained in section 3.2 for scattering of continuous wave signals from nonstationary surfaces, it is apparent that with the substitution $T/\alpha = \Delta x$, the two expressions are identical. It thus follows that the results presented in figures 4 - 6 for the scintillation index are applicable also to the backscatter of Gaussian weighted pure tone pulses.

To compute the time-lagged intensity covariance, expressions are needed for $< p(t)p^*(t) >$ and $< p(t')p^*(t') >$ or for $< I(\tau_s \pm \Delta t/2) >$. For the pure tone pulse (20)

$$< I(\tau_s \pm \Delta t/2) >= (2\pi|F|)^2 \int d\vec{\rho}_+ \widehat{W}_B(\vec{\rho}_+) \tag{21}$$

$$\times \exp[-2y_+^2/(\Delta y)^2 - 2x_+^2\alpha^2/T^2 \pm 2\Delta t x_+ \alpha/T^2 - (\Delta t)^2/(2T^2)]$$

Taking an ensemble average over all nonstationary surface representations

$$< \overline{I(\tau_s \pm \Delta t/2)} >= 2\pi^3|F|^2\Delta y(T/\alpha)\widehat{W}_B$$

yields a result that is independent of time, where $\widehat{W}_B = \overline{\widehat{W}_B(\vec{\rho}_+)}$.

Because the results presented in section 3 display only a weak dependence on the form of the correlation function assumed for $\overline{W_B(\vec{\rho}_+)W_B(\vec{\rho}_+')}$ in (12), a Gaussian correlation function (13) will be assumed. For the Gaussian case, the first term contributing to the time-lagged intensity covariance (15) takes the form

$$< \overline{I(\tau_s + \Delta t/2) >< I(\tau_s - \Delta t/2)} >= (2\pi^3|F|^2\widehat{W}_B\Delta y T/\alpha)^2$$

$$\times\{1 + \gamma' \exp[-(\Delta t/\alpha L_W)^2/(1 + T^2/\alpha^2 L_W^2)]\} \tag{22}$$

where γ' is defined as

$$\gamma' = \gamma[1 + (\Delta y/L_W)^2]^{-1/2}[1 + (T/\alpha L_W)^2]^{-1/2}$$

For a stationary surface, this contribution to the intensity covariance is independent of lag time. In the case of nonstationary surfaces, a time dependence is predicted that depends strongly on the characteristic patch size L_W. A result of this general form was first obtained by Crowther [1980].

Using approximation (19), the second contribution to the time-lagged intensity covariance is

$$\overline{|<p(\tau_s+\Delta t/2)p^*(\tau_s-\Delta t/2)>|^2}=(2\pi^3|F|^2\widetilde{W}_B\Delta yT/\alpha)^2(1+\gamma')\exp[-(\Delta t)^2/T^2] \quad (23)$$

The dependence of this contribution to the intensity covariance on lag time is the same for both stationary and nonstationary surface statistics, the only difference in the two cases being the scale factor $1+\gamma'$. On comparing (22) and (23), it is evident that the nonstationary contribution of (22) decays more slowly with lag time than that of (23) and hence provides a means of estimating L_W.

Assuming that the wave-number spectrum in (22) is a slowly varying function of K_x, $\widehat{W}_B$ in this expression may be replaced by $\widetilde{W}_B$. We then consider the normalized time-lagged intensity covariance $\mathcal{C}(\Delta t)$ where

$$\mathcal{C}(\Delta t)=<\overline{I(\tau_s+\Delta t/2)I(\tau_s-\Delta t/2)}>/[\overline{<I(\tau_s)>}]^2$$

In figure 8, the normalized intensity covariance is shown as a function of lag time for stationary and nonstationary surfaces. This figure presents predictions for a slant range of 50 m, grazing angle of 30°, and horizontal beamwidth of 10°. Results are shown for a pulse length of 1 msec, for three characteristic patch sizes. For the value of $\gamma = .5$ and the scattering geometry assumed in this figure, only for $L_W = 5$ m, will the slowly varying time dependent factor in (22) be clearly apparent, given that the validity of these results requires $\Delta t \ll \tau_s$.

Figure 9 shows the normalized intensity covariance predicted for a scattering geometry of larger scale in which a slant range of 500 m and pulse length of 10 msec are assumed. A horizontal beamwidth and grazing angle of 10° were used to obtain results for a stationary surface $\gamma = 0$ and a nonstationary surface with $\gamma = 1$. For this pulse length, nonstationary features having a charateristic length $L_W < 5$ m are not experimentally resolvable. However, the decay of the covariance due to large scale nonstationary features permits an estimation of L_W in such cases.

4.2. Spectral representation of nonstationary processes

While the examples presented in figures 9 and 10 provide some insight into the dependence of the intensity covariance on experimental and seafloor parameters, they entail the assumption that C_W depends on a single length scale L_W. A more general form for this correlation function is

$$C_W(\vec{\rho}) = \int d\vec{K} S(\vec{K}) \exp i\vec{K} \cdot \vec{\rho}$$

For a pure tone pulse, the contribution to the intensity covariance of (22) then takes the form

$$< \overline{I(\tau_s + \Delta t/2)} >< I(\tau_s - \Delta t/2) >= (2\pi^3 |F|^2 \widehat{W}_B \Delta y T/\alpha)^2$$

$$\times \{1 + (\gamma/4\pi^2) \int d\vec{K} S(\vec{K}) \exp[-K_y^2 (\Delta y)^2/4 - K_x^2 T^2/4\alpha^2 + iK_x \Delta t/\alpha]\} \qquad (24)$$

With the change of variables $\Delta t = 2\Lambda/c$, (24) may be Fourier transformed with respect to Λ via $\mathcal{F}(\kappa_x) = \int d\Lambda \exp(-i\kappa_x \Lambda) f(\Lambda)$. Assuming a record of sufficient length, there results

$$\mathcal{F}(\kappa_x) = (\gamma \alpha c/4\pi)(2\pi^3 |F|^2 \widehat{W}_B \Delta y T/\alpha)^2 \int dK_y S(\alpha c \kappa_x/2, K_y)$$

$$\times \exp[-c^2 T^2 \kappa_x^2/4 - K_y^2 (\Delta y)^2/4] \qquad (25)$$

This procedure thus provides a damped and averaged estimate of the spatial decomposition of C_W. For (25) to provide a reliable estimate of $S(K_x, 0)$, it is required that $\Delta y > \Lambda_{max}$ where Λ_{max} is the maximum length scale of interest so that averaging effects will be unimportant. In addition, for the rolloff with increasing κ_x in (25) to be negligible, we require $T < \Lambda_{min}/\pi c$ where Λ_{min} is the minimum length scale of interest.

Chotiros, et al [1985] Fourier transformed detrended intensity records and obtained results that differ from predictions [McDaniel 1990] for 1 m $< \Lambda <$ 10 m. Their data were acquired using a pulse length of 1 msec and $\Delta y \approx 3.5$ m, so that neither of the criteria above are fulfilled, and the data cannot be inverted to estimate $S(K_x, 0)$.

4.3. Frequency diversity

In both microwave and optical scattering from rough surfaces a frequency diversity or frequency averaging effect has been experimentally observed [Ulaby et al 1988, George and Jain 1972]. For backscatter this effect can be characterized by the parameter $N \approx 2D\Delta f/c$ [Ulaby et al] where D is the slant-range resolution of the detection system, and Δf is the bandwidth of the transmitted waveform. Experiments employing broadband signals have been used to verify that $\sigma^2 \approx 1/N$ for scattering from sufaces that are homogeneous on the scale of the sensor's footprint, so that as the signal bandwidth is increased from its nominal value for a pure tone pulse $\Delta f = 1/T$, the scintillation index decreases. It is of interest to determine if such an effect is predicted in the case of Bragg backscatter.

First let us consider scattering from statistically stationary surfaces. If (15) is valid then

$$< I^2(t) > \equiv 2 < I(t) >^2$$

so that $\sigma^2 \equiv 1$ regardless of the transmitted waveform and no frequency diversity effect is predicted. The validity of (15) requires that the dimensions of the scattering area be large on the scale of the wavelength of the ensonifying signal and that the surface roughness wave-number spectrum vary slowly in the vicinity of the Bragg wave number so that the scattering process is highly wave-number selective. Recall also that (15) is valid irrespective of the frequency independent assumption.

For scattering from nonstationary rough surfaces, we invoke approximation (19) and assume a waveform

$$e(t) = \exp[i(\omega_0 t + bt^2) - t^2/T^2]$$

It may be readily verified that in this case the result obtained is independent of the choice of the parameter b so that the results reduce to those obtained for the pure tone pulse of (20) and again a frequency diversity effect is not predicted. In this case, two additional assumptions have been made: that the scatter is frequency independent, and that the approximation of (17) by (18) is valid.

It is appropriate at this point to examine in detail the validity of approximation (18). For a pure tone pulse, (17) and (18) may be integrated assuming wave-number spectra of Gaussian and power-law form. In the Gaussian case (17) yields a dependence on Δt of the form $\exp[-(\Delta t)^2/2(T^2+2\alpha^2L^2)]$ while approximation (18) yields a dependence $\exp[-(\Delta t)^2/2T^2]$. It is clear that only if $T \gg \alpha L$ is (18) valid for this assumed form of the wave-number spectrum. Results are shown for the power-law spectrum of (11) in figure 10, for a slant range of 50 m, grazing angle of 30°, horizontal beamwidth of 10° and frequency of 10 kHz. The three curves shown are the normalized level predicted by (18), the relative magnitude of the predictions of (18) to those of (17), and the difference in phase between the predictions of (18) and (17). It is evident that for the power-law wave-number spectrum, approximation (18), and hence (19), is valid even for the values of $T = 1$ msec and $L = 100$ m, used in this example, for which $T < \alpha L$. Thus, within the additional limitation imposed by the frequency independent assumption, no diversity effect is predicted for scatter from nonstationary rough surfaces.

The reason for the lack of a frequency diversity effect for the Bragg backscattering processes addressed in this study is not intuitively evident. It is thus worthwhile seeking a simple physical explanation for this finding. In the case of point scatterers, the diversity effect occurs because each irradiated scatterer returns a replica of the transmitted pulse. For Bragg scatter, however, the scatter at frequency ω_1 is governed by surface features having a wave number $K_x = \alpha\omega_1$, and at frequency ω_2 by those having a wave number $K_x = \alpha\omega_2$. Thus, in the case of Bragg backscatter, frequency diverse waveforms increase the effective number of "scatterers", which has no effect since this number is already large. For the same reason, the effects of frequency diversity may not be fully realized for other resonant scattering processes, such as scatter from the resonant microbubbles that are responsible for high-frequency sea surface backscatter.

Frequency averaging effects have been experimentally observed for both volume scatter and backscatter from rough surfaces at elevated grazing angles. Thus, the absence of a

frequency diversity effect is an important feature of Bragg scattering processes permitting their clear identification. It is noteworthy that the results of two experiments reported by Chotiros, et al [1985] and Boehme and Chotiros [1988], where the parameter N took on values of one and four at both sites where measurements were conducted, display no dependence of the scattered field statistics on the bandwidth of the transmitted waveform.

5. Comparison with experiment

The data with which the theoretical predictions will be compared were acquired by Gensane [1989] at two sites in an area characterized by a sandy seafloor. At one of the sites, the seafloor was described as flat, while at the second, sand ripples with a spatial period of 1.2 m were observed. A parametric source having a nominal horizontal beamwidth of 3° at the frequencies of interest was used in these measurements which were conducted along four bearings at each site. The height of the projector above the seabed was adjusted so that the slant range to the ensonified area varied between 20 and 40 m. The projected signals were selected to obtain data for a wide range of frequencies, pulse lengths, and signal bandwidths.

Our interest is in the pulse length dependence of the scintillation index reported for gated pure tone pulses at frequencies of 20 and 40 kHz over the grazing angle range of 4 to 20°. These indices were determined by first analyzing the data to determine the scattering strength and then detrending the data to remove the general dependence of the scattering strength on grazing angle, a procedure described in detail by Chotiros, et al [1985]. Further analysis was then performed to determine the probability distribution and various moments of the detrended data.

The measured scintillation indices shown in figure 11 represent an average over the data at the two sites. The data for pulse lengths of .25 and 1 msec were acquired at a frequency of 40 kHz. The 20 kHz data plotted for a pulse length of 1.5 msec is the reported average of scintillation indices measured using 1 and 2 msec pulses. The theoretical curves presented for comparison assume C_W of (12) is Gaussian, in which case

$$\sigma^2 = 1 + 2\gamma[1 + (T/\alpha L_W)^2]^{-1/2}[1 + (\Delta y/L_W)^2]^{-1/2}$$

for a Gaussian weighted pure tone pulse, and it is assumed that this expression is applicable for a gated pure tone of duration equal to the effective pulse length of the Gaussian weighted pulse. An average slant range of 30 m and grazing angle of 12° were used in evaluating σ^2.

As is evident with the logarithmic time scale employed in figure 11, σ^2 exhibits a "knee" whose position is strongly dependent on the characteristic patch size L_W assumed, and to obtain agreement with the data $L_W \approx 1$ m. With the position of this knee established, $\gamma \approx 1.5$ follows from matching the magnitude of σ^2. Variations of this magnitude in the wave-number spectrum over short ranges are consistent with the observations of Briggs [1989].

While the value of γ derived from Gensane's data is in agreement with values found by Crowther [1980], the characteristic length L_W in this case differs greatly from the typical value of 100 m found by Crowther. This difference may be due, in part, to the 10 msec pulse lengths employed in Crowther's measurements which yield insufficient resolution to observe fluctuations on the scale of a meter. On the other hand, in Gensane's case, the very limited range scale of the measurements prevents observation of large patches.

6. Discussion

A theory of backscattering from slightly rough statistically nonstationary surfaces has been developed and applied to the seafloor reverberation process. The validity of the analysis requires only that the dimensions of the ensonified area be large on an acoustic wavelength scale and that the surface roughness wave-number spectrum be slowly varying near the Bragg wave number — conditions that are satisfied for seabed reverberation. Under these two conditions, the scintillation index predicted for scattering from statistically stationary surfaces is unity, so that nonstationarity must be invoked to obtain agreement with experiment. The theory is applicable as well to microwave scattering from the sea surface and could be employed to investigate such effects as the influence of ripple near wave crests [Longuet-Higgins 1987] on the statistics of sea clutter.

When the theory is extended to the time domain, another feature of Bragg scatter becomes apparent: that the frequency diversity effect observed for volume scatter and scatter

from very rough surfaces at high grazing angles is absent. This is of importance for seafloor reverberation because it may provide a method of distinguishing the contributions of rough surface scatter from those of scattering due to volume inhomogeneities within the seabed.

In this analysis, the modified reflection coefficient $\chi(\theta)$ of (4) has been treated as a constant. However, nonstationarity of this parameter could contribute significantly to the experimentally observed fluctuations. A theory comparable to that developed here that includes variations in χ would contain a strength parameter γ_χ equal to the normalized variance of $|\chi|^2$. A crude estimate of this variance may be made using the variances of sound speed and density reported by Jackson and Briggs [1992] and Yamamoto [1995]. Assuming that the seabed may be treated as a homogeneous halfspace with correlated laterally varying parameters, for sandy sediments γ_χ is estimated to be on the order of unity below the critical angle and significantly lower above this angle. This estimate suggests that, if sound speed and density variability is a contibuting factor, the fluctuation statistics will decrease with increasing grazing angle. Only Crowther [1980] reports such a dependence of fluctuation statistics on grazing angle. For sands, surficial sediment layering [McDaniel 1992] and sound speed gradients [Moe and Jackson 1994] may strongly effect χ at grazing angles above the critical angle. Lateral variation of these parameters would hence produce an increase in fluctuation with grazing angle. It is evident from this brief discussion that careful studies are needed to fully assess the contribution of sediment variability to reverberation fluctuations.

Acknowledgement

This research was supported by the Office of Naval Research.

References

Boehme H and Chotiros N P 1988 Acoustic backscattering at low grazing angles from the ocean bottom *J. Acoust. Soc. Am.* **84** 1018-29

Briggs K B 1989 Microtopographical roughness of shallow-water continental shelves *IEEE J. Oceanic Eng.* **14** 360-7

Chotiros N P, Boehme H, Goldsberry T G, Pitt S P, Lamb R A, Garcia L and Altenburg R A 1985 Acoustic backscatter at low grazing angles from the ocean bottom. Part II Statistical characteristics of bottom backscatter at a shallow water site *J. Acoust. Soc. Am.* **77** 975-82

Crowther P A 1980 Fluctuation statistics of sea-bed acoustic backscatter in *Bottom-Interacting Ocean Acoustics* eds W A Kuperman and F B Jensen (Plenum, New York)

Fox C G and Hayes D E 1985 Quantitative methods for analyzing the roughness of the seafloor *J. Geophys. Res.* **23**

Gensane M 1989 A statistical study of acoustic signals backscattered from the sea bottom *IEEE J. Oceanic Eng.* **14** 84-93

George N and Jain A 1972 Speckle in microscopy *Opt. Commun.* **6** 253-7

Goff J and Jordan T 1988 Stochastic modeling of seafloor morphology: Inversion of Sea Beam data for second-order statistics *J. Geophys. Res.* **93** 13589-608

Goodman J W 1976 Some fundamental properties of speckle *J. Opt. Soc. Am.* **66** 1145-50

Gradshteyn I S and Ryzhik I M 1980 *Table of Integrals, Series and Products* (Academic Press, New York)

Jackson D R, Winebrenner D P and Ishimaru A 1986 Application of the composite roughness model to high-frequency bottom backscattering *J. Acoust. Soc. Am.* **79** 1410-22

Jackson D R and Briggs K B 1992 High-frequency bottom backscattering: Roughness versus sediment volume scattering *J. Acoust. Soc. Am.* **92** 962-77

Jakeman E and Pusey P N 1976 A model for non-Rayleigh sea clutter *IEEE Trans. Antennas Propag.* **24** 806-14

Kur'ynov B F 1963 The scattering of sound waves at a rough surface with two types of irregularity *Sov. Phys. Acoust.* **8** 252-7

Longuet-Higgins M S 1987 The propagation of short surface waves on longer gravity waves *J. Fluid Mech.* **177** 293-306

McDaniel S T 1990 Seafloor reverberation fluctuations *J. Acoust. Soc. Am.* **88** 1530-5

McDaniel S T 1992 Effect of surficial sediment layering on high-frequency seafloor reverberation *J. Acoust. Soc. Am.* **91** 1353-6

Melton D R and Horton C W 1970 Importance of the Fresnel correction in scattering from a rough surface. I. Phase and amplitude fluctuations *J. Acoust. Soc. Am.* **47** 290-303

Moe J E and Jackson D E 1994 First-order perturbation solution for rough surface scattering cross section including the effects of gradients *J. Acoust. Soc. Am.* **96** 1748-54

Oliver C J 1984 A model for non-Rayleigh scattering statistics *Optica Acta* **31** 701-22

Ol'shevskii V V 1967 *Characteristics of Ocean Reverberation* (Plenum, New York)

Papoulis A 1965 *Probability, Random Variables and Stochastic Processes* (McGraw-Hill, New York)

Ulaby F A, Haddock T F and Austin R T 1988 Fluctuation statistics of millimeter-wave scattering from distributed targets *IEEE Trans. Geosci. Remote Sensing* **26** 268-81

Valenzuela G R and Laing M B 1970 On the statistics of sea clutter U S Naval Res. Lab. Rep. NRL-7349

Yamamoto T 1995 Velocity variables and other physical properties of marine sediments measured by crosswell acoustic tomography *J. Acoust. Soc. Am.* **98** 2235-48

Yang C C, Fennemore G C and McDaniel S T 1992 Scintillation index of the acoustic field forward scattered by a rough surface for two-and three-dimensional scattering geometries *J. Acoust. Soc. Am.* **91** 1960-6

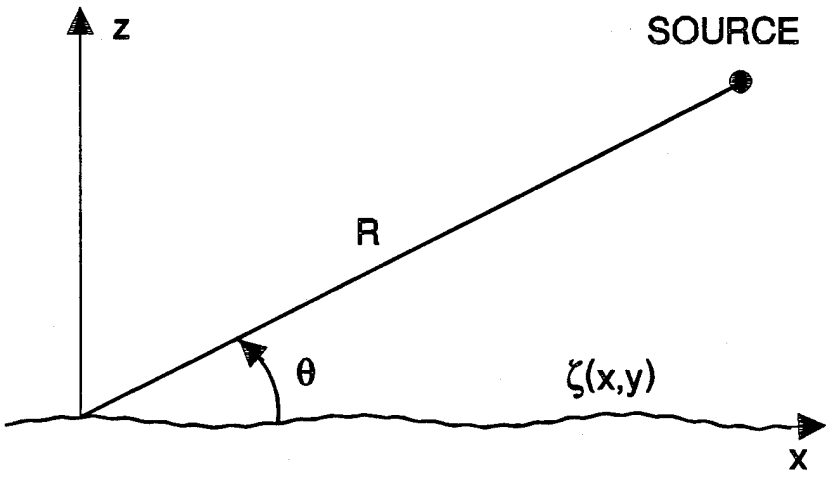

Figure 1. Geometry for backscattering from a random rough surface.

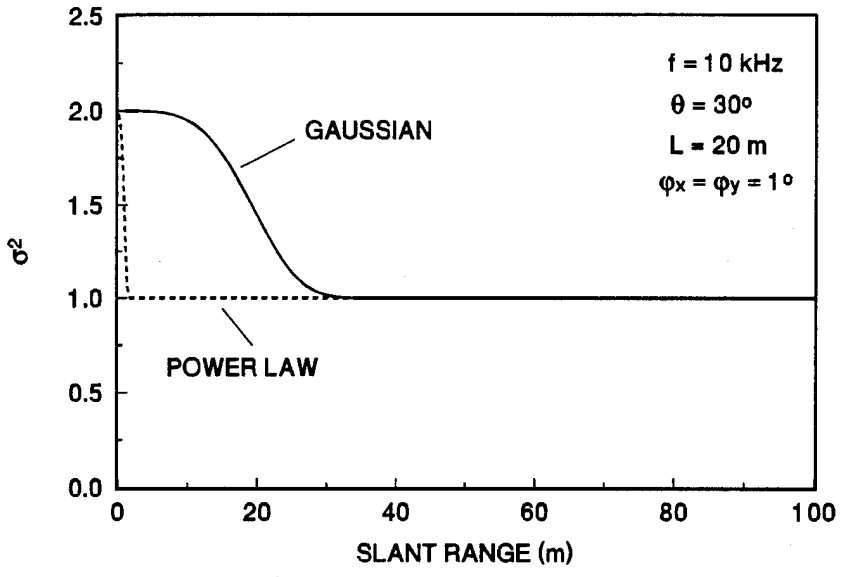

Figure 2. Scintillation index for scatter from statistically stationary surfaces having Gaussian and power-law wave-number spectra.

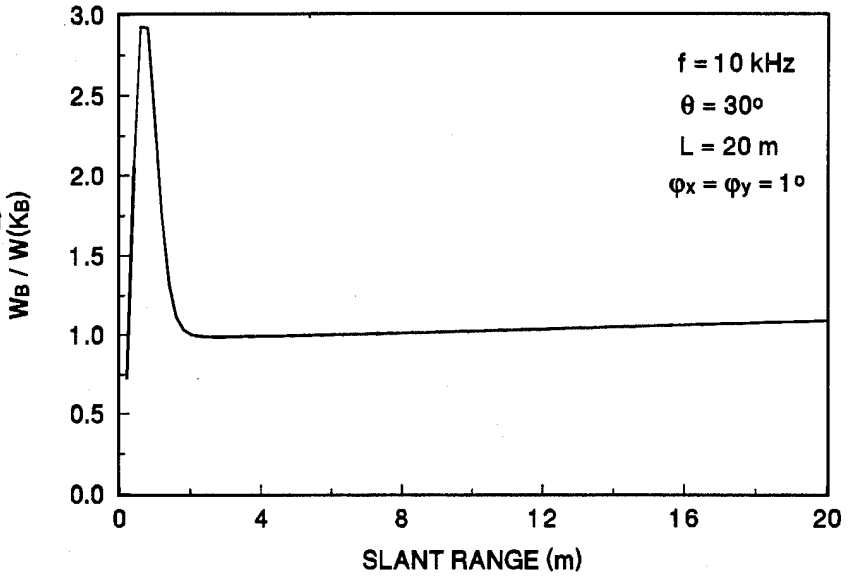

Figure 3. Ratio of the scattered intensity to that predicted at the Bragg frequency for scatter from a stationary rough surface characterized by a power-law wave-number spectrum.

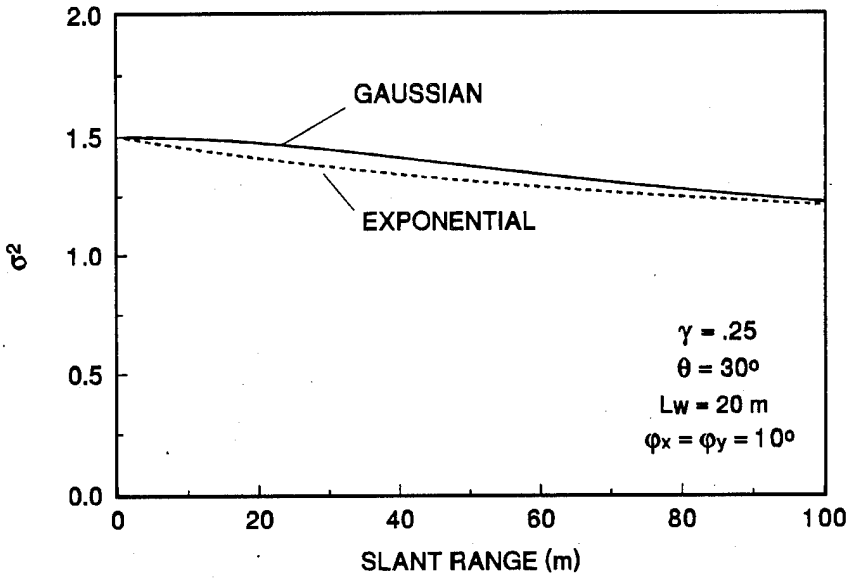

Figure 4. Scintillation index for scattering from rough surfaces having Gaussian and exponentially correlated nonstationarity with a characteristic length of 20 m.

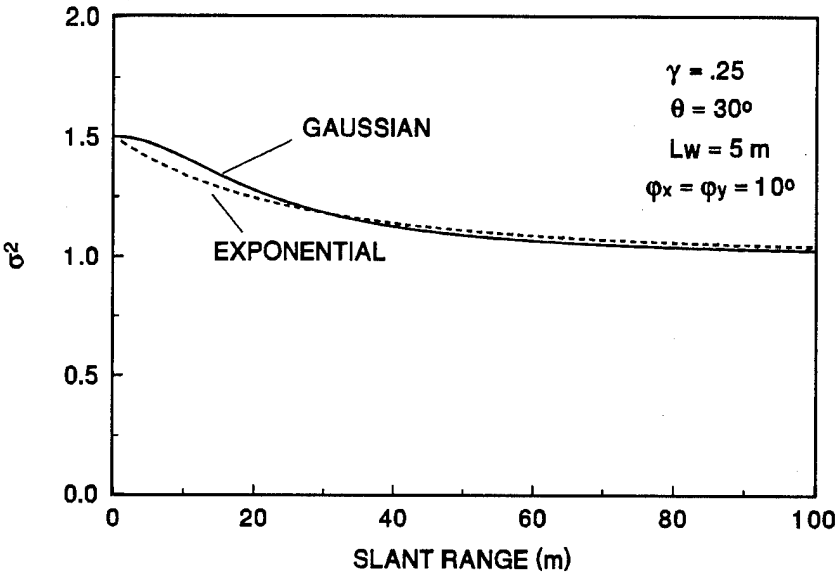

Figure 5. Scintillation index for scattering from rough surfaces having Gaussian and exponentially correlated nonstationarity with a characteristic length of 5 m.

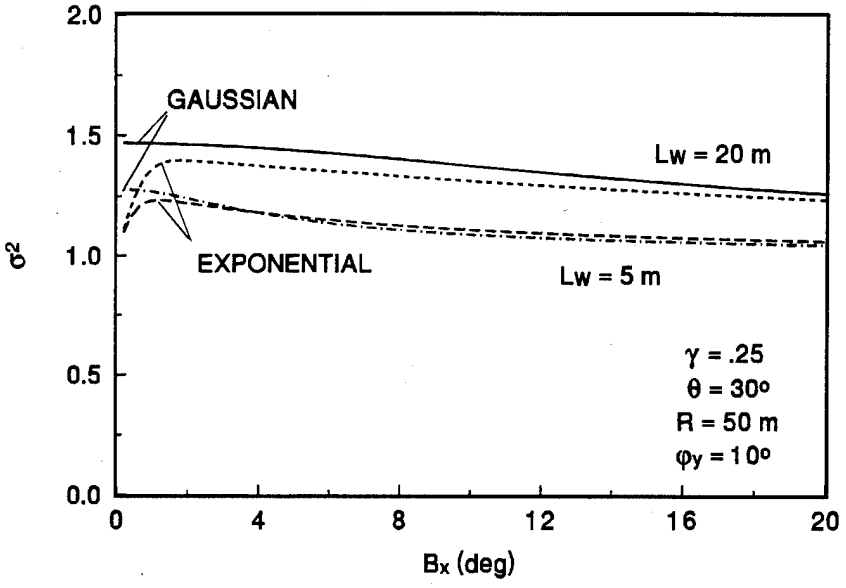

Figure 6. Dependence of the scintillation index on beamwidth for scattering from rough surfaces having Gaussian and exponentially correlated nonstationarity with characteristic lengths of 5 and 20 m.

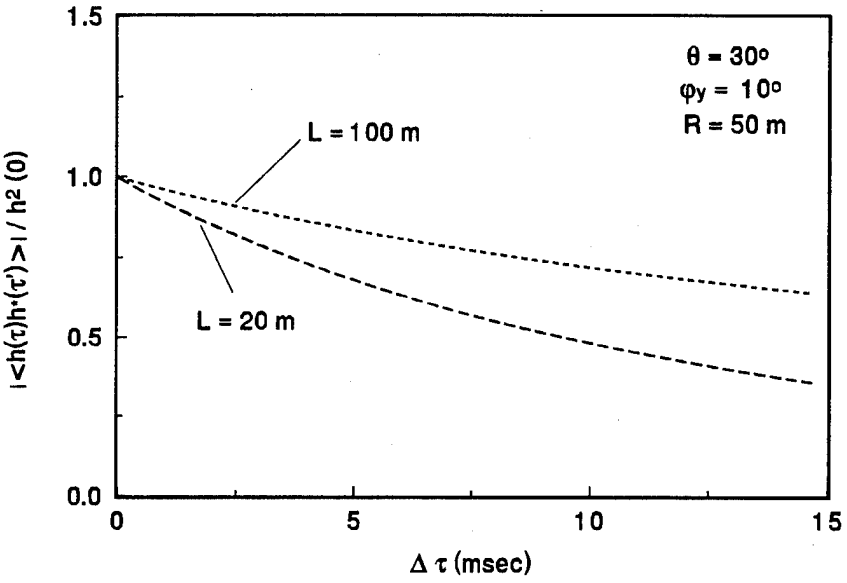

Figure 7. Normalized temporal covariance of the impulse response for scatter from a rough surface having power-law wave-number spectra with characteristic lengths of 20 and 100 m.

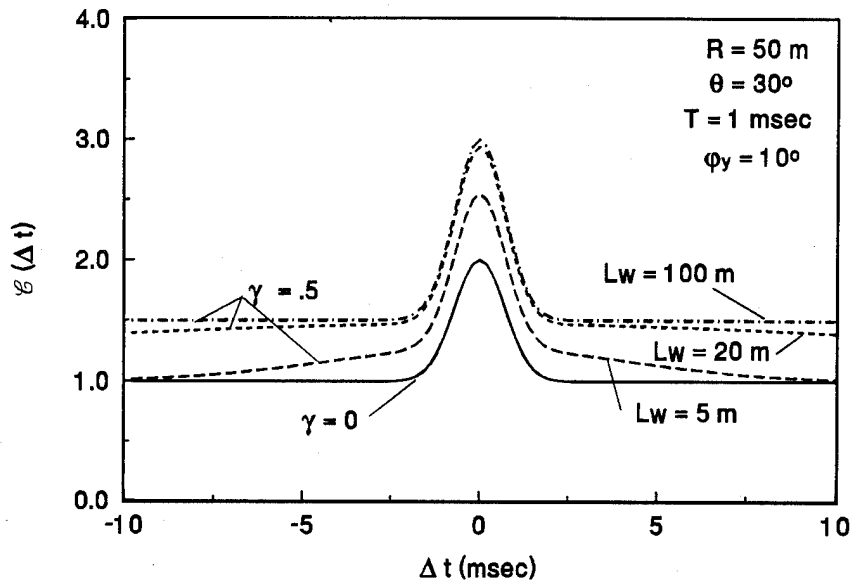

Figure 8. Normalized temporal intensity covariance for the scatter of a 1 msec pure tone pulse from a stationary rough surface and surfaces having Gaussian correlated nonstationarity with characteristic length as a parameter.

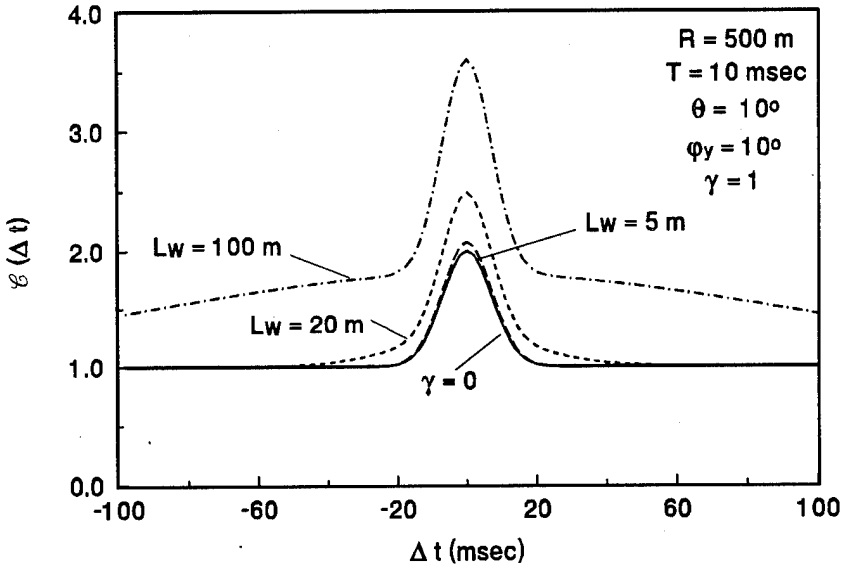

Figure 9. Normalized temporal intensity covariance for the scatter of a 10 msec pure tone pulse from a stationary rough surface and surfaces having Gaussian correlated nonstationarity with characteristic length as a parameter.

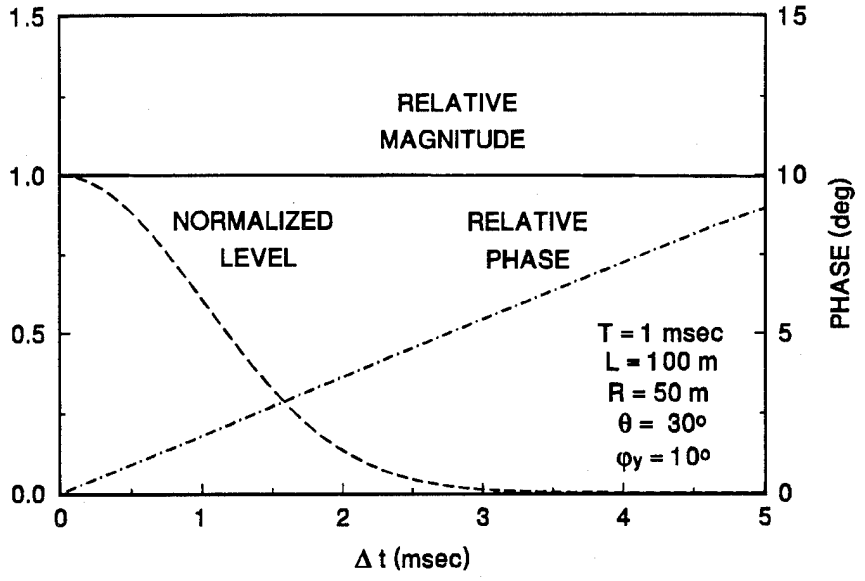

Figure 10. Relative predictions of $< p(\tau_s + \Delta t/2)p^*(\tau_s - \Delta t/2) >$ by (17) and its approximation (18) for the scatter of a 1 msec pure tone pulse from a rough surface having a wave-number spectrum of power-law form with a characteristic length of 100 m.

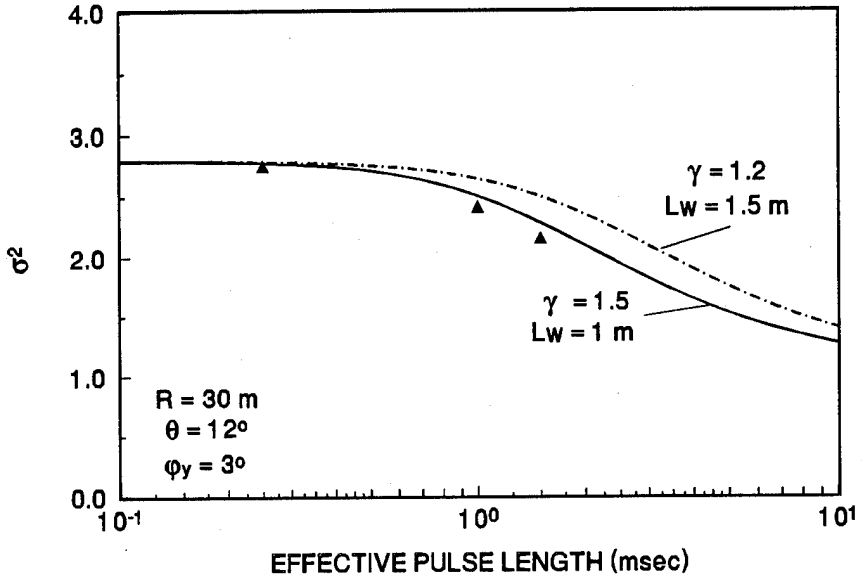

Figure 11. Comparison of measured scintillation indices as a function of effective pulse length with predictions assuming Gaussian correlated nonstationarity.